

Deep learning based vertebral scale prediction for ultrasound-accessible landmark registration-based visualizations of diseased spines

Ben Church¹, Andras Lasso¹, Christopher Schlenger²,
Daniel P. Borschneck³, Parvin Mousavi⁴, Gabor Fichtinger^{1,3}, Tamas Ungi^{1,3}

1. Laboratory for Percutaneous Surgery, School of Computing,
Queen's University, Kingston, ON, Canada
2. Premier Chiropractic, Stockton, CA, USA
3. Department of Surgery, Queen's University, Kingston, ON, Canada
4. Medical Informatics Laboratory, School of Computing,
Queen's University, Kingston, ON, Canada

ABSTRACT

The safety, inexpensiveness, and accessibility of ultrasound imaging has caused it to gain research interest as a tool for intra-operative spinal navigation over traditional fluoroscopy or CT imaging. The difficulty of interpreting ultrasound images, however, has caused resistance to it being adopted for widespread clinical use. This problem can be remedied if pre-operative a CT segmentation, or statistically derived spine atlas are registered to the intra-operative, spatially tracked ultrasound images. There are a number of methods in literature for accomplishing this, however pre-operative CT scans reintroduce the problem of ionizing radiation, and it is challenging to produce statistical atlases for spines exhibiting abnormal anatomic geometry, such as in cases of scoliosis. We propose a method for registering a healthy-shaped spine model to abnormal patient anatomy using the ultrasound-accessible transverse process locations as input. Our method constrains the registration with anchor points, the locations of which are computed with input from deep learning models' predictions of other anatomic landmark locations, such that they scale each of the healthy model's vertebrae to those of the patient. Average and maximum Hausdorff distances between the registrations and CT segmentations were calculated to assess the registration accuracy. Registrations were also generated with a similar method which computes vertebral scale based on distances between adjacent transverse processes, averaged across the entire spine. This serves to illustrate the improvements in registration which can be achieved by using deep learning to predict aspects of patient anatomy from limited information, in this case, the transverse process locations.

1 Introduction

Lumbar spine injections are widely used to deliver pain relief to patients suffering from facet joint pain, and for epidural anesthesia during labor. The target injection site's size, depth, and proximity to the spinal cord and nerves make these procedures challenging, often requiring multiple insertion attempts and causing nerve damage. The difficulty and risks associated with such injections have caused fluoroscopy and CT to emerge as the standard imaging modalities for guiding these procedures. However, fluoroscopy and CT imaging result in repetitive exposure of practitioners to ionizing radiation. The health and safety standards made necessary by the risks associated with these imaging techniques increase their cost, and decrease their availability.

The safety, low cost, and accessibility of ultrasound imaging has attracted research investigating it as an alternative imaging modality for guiding a these procedures. Loizides et al. [Loizides2011] present a method for locating lumbar injection sites using ultrasound. Ungi et al. [Ungi2012b] extend basic ultrasound by adding spatial tracking to the ultrasound and needle, allowing images to be captured, and the needle positioned without the need to manage the probe simultaneously. Despite these methods allowing for the location of injection sites without ionizing radiation, they have not gained widespread use, partly due to the difficulty of interpreting ultrasound images. Addressing this difficulty, more recent work by Nagpal et al. [Nagpal2015] and Zettinig et al [Zettinig2016], investigated generating 3D surface visualizations of patient spines by registering CT-derived surface models to patients' tracked ultrasound

scans. However, the need for a CT scan of the patient to register makes these methods unsuitable for reducing radiation exposure.

Behnami et al [Behnami2016] and Seitel et al. [Seitel2016] generated similar visualizations, but by registering statistical atlas spine models to patient ultrasound, eliminating the need for prior CT scans, and ionizing radiation with them. Statistical atlas registration is feasible in cases where the geometry of the spine is normal, as the availability of previous CT scans of such spines provides enough data to generate the atlas. This is not the case in states of disease causing abnormal geometry, such as scoliosis. The wide variety of shapes possible in diseased spines makes the collection of sufficient data to generate an atlas challenging. [Anon2017] presented a method for generating surface visualizations of spines by deforming a generic, healthy-shaped spine model to patient anatomy, based on only the patient's transverse process locations. [Anon2017] produced qualitatively informative visualizations, testing their method on four patients, however the visualization accuracy was not validated for interventional navigation.

The method developed by [Anon2017] addresses the challenge of conveying the anterior-posterior scale of patients' vertebrae in a thin-plate spline registration by adding anchor points to the manually located transverse process landmarks. The anchor points are added towards the vertebral bodies from the transverse processes, distributing points in the anterior-posterior direction, which otherwise lacks constraint. They computed this direction by cross-producing vectors pointing from landmarks on one vertebra, to corresponding landmarks on adjacent vertebrae, with vectors pointing from one landmark to its symmetric partner on the same vertebra. The magnitude of these cross-products was the distance between corresponding landmarks of adjacent vertebrae, averaged over the entire spine. This conveyed the scale of the patient's anatomy in the registration landmarks, relative to that of the healthy-shaped model. However, individual vertebrae are subject to scale variability, especially in cases of abnormal anatomy, such as the scoliotic patients of their study.

There remains the need for a method which produces spinal visualizations for interventional guidance without using ionizing radiation, and which is suitable for cases of abnormal anatomic geometry and variable vertebral scale. We address this need in the remainder of the paper, which is organized as follows. We present an improved version of the method from [Anon2017]. Our method improves registration results by using deep learning to predict vertebral scales, whereas their method relied purely on patient-wise average inter-landmark distances for registration scale estimation. We present average and maximum Hausdorff distances between our registrations and CT-derived ground-truth models, demonstrating the quantitative improvement our method offers. We illustrate the improvements qualitatively by comparing registrations produced by both methods and discuss these results.

2 Methods

Like in [Anon2017], a healthy-shaped spine model was deformed to patient anatomy based on a thin-plate spline registration between model and patient landmarks. Anchor points were added to the transverse process locations to constrain the registration in the anterior-posterior direction, and convey rotation about the axes of the vertebrae. The directions in which the anchor points were added to their corresponding transverse processes were calculated using the previous cross-product method. The transverse process locations are shown in red with yellow anchor points in Figure 1. Whereas [Anon2017] used patient-wise average inter-landmark distances to compute the magnitude of the distance between the anchor points and their corresponding transverse processes, our method computes these distances for each vertebra individually. To convey vertebral scale in this distance, we incorporate landmarks on the anterior faces of vertebral bodies. Since these landmarks cannot be located using ultrasound, their locations were predicted using deep learning, based on the ultrasound-accessible transverse process locations.

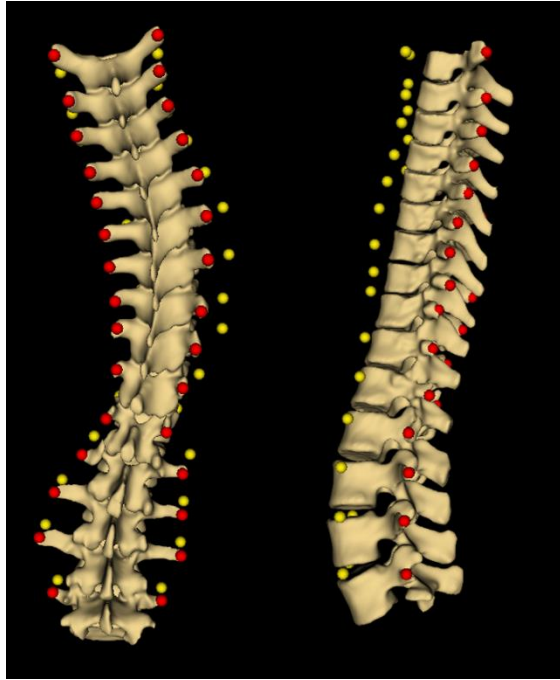


Figure 1: Posterior and left views of a patient's spine showing transverse process landmarks in red and anchor points in yellow

the spines by extrapolation from existing landmarks. The average of the two vectors pointing from the transverse process landmarks of the vertebrae just inside the boundaries, to the corresponding landmarks on the boundary vertebrae were computed. Points were added outside the boundaries at offsets equal to these vectors, allowing the boundary scale points to be predicted.

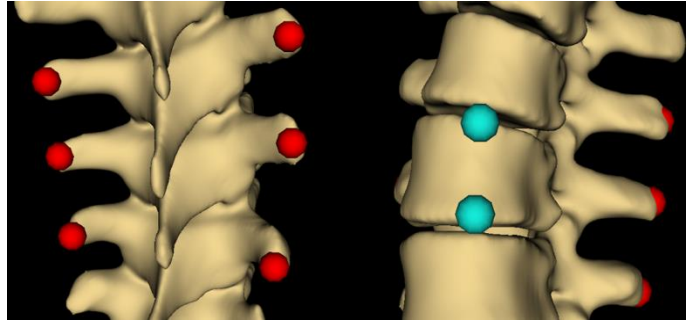


Figure 2: Left: Six 3D transverse process locations constituting one 18 dimension input vector to the deep learning model. Right: Two 3D scale point locations, the target output for the model.

H2O's (www.h2o.ai) deep learning models were used to predict the locations of the top and bottom edges of the left-right centers of the anterior faces of the vertebral bodies for each patients' vertebrae. The locations of the transverse processes from three vertebrae, centered about the vertebra for which the predictions were being made, were used as input to our models. One input instance and its corresponding target output are shown in Figure 2. Since the superior and inferior-most vertebrae of the patients' spines have only one neighboring vertebra, boundary conditions arise. These boundaries were addressed by adding a transverse process pair above and below

the deep learning model's feedforward architecture is shown in Figure 3. The six 3D landmark points were input as 18 dimensional vectors, used to predict the location of the given vertebral body point. H2O does not currently support multiregression problems, therefore a model was trained for each of the two vertebral body points' coordinates. 116 patient's transverse processes and vertebral bodies were marked. 13 of these were set aside to test the model, after it was trained on the remaining 103 patients providing a total of 1122 input vectors. Each of the models' was trained with 5-fold cross-validation for 10 epochs, with 0.1 for both input dropout and L2 regularization.

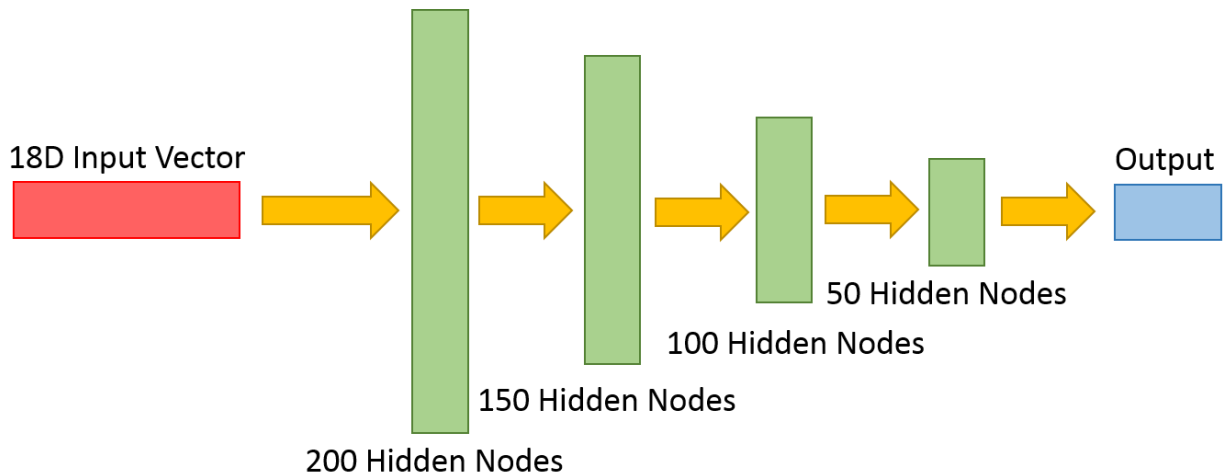


Figure 3: Deep learning architecture

Once the models were trained, they were used to predict each coordinate of the 13 remaining patients' vertebral body points. Both the transverse process points and the predicted vertebral body points were used to estimate the anterior-

posterior scale of a vertebra as follows: The average position of the vertebra's transverse processes was calculated, as was the average of the two vertebral body points. The vector pointing from the one averaged location to the other was then computed. The length of this vector, excluding the superior-inferior component was computed and used as the magnitude of the distance between the vertebra's transverse processes and their corresponding anchor points. The superior-inferior component was excluded because the wide distribution of points in this direction made its predictions inaccurate.

Once the magnitudes of the distances between the transverse processes and their anchor points were calculated, the anchor points were added and the registration performed as in [Anon2017]. The CT segmentations used to locate the transverse processes were used as ground-truths to assess the accuracy of the registrations. Maximum and average Hausdorff distances were calculated for these registrations and ones using the method originally described in [Anon2017]. Minimum distances between the registrations and ground-truth surfaces were calculated and displayed on the registrations as error maps, several cases of interest we show in the following results section.

3 Results

Table 1 shows both the average and maximum Hausdorff distances for registrations produced using the patient-wise average scaling method from [Anon2017], and from our deep learning vertebra-wise scaling method.

Patient #	Patient-wise scaling		Vertebra-wise scaling	
	Avg. Hausdorff (mm)	Max. Hausdorff (mm)	Avg. Hausdorff (mm)	Max. Hausdorff (mm)
1	2.8	20.2	2.2	18.3
2	2.3	23.5	2.9	23.5
3	2.5	16.6	2.4	16.6
4	3.0	19.0	2.1	15.2
5	2.6	15.8	2.4	17.9
6	3.4	18.6	2.4	15.1
7	3.0	22.4	2.4	21.0
8	3.1	21.5	1.8	16.0
9	3.4	23.4	2.8	23.6
10	2.2	20.1	2.1	20.6
11	2.5	16.6	1.5	14.1
12	3.0	20.5	2.5	28.4
13	2.7	18.1	2.3	16.8
Mean (mm)	2.8	19.7	2.3	19.0
Standard deviation (mm ²)	0.4	2.6	0.4	4.2

Table 1: Average and maximum Hausdorff distances comparing the method using patient-wise scaling from [Anon2017] to current the method using vertebra-wise scaling

Several notable registrations are those of patient #2, whose average Hausdorff distance increased, and patient #12, whose maximum Hausdorff distance increase under the vertebra-wise scaling method. Patients #8 and #11 are also interesting for their distinct improvements in their average Hausdorff distances. Error maps are shown over these registrations for both methods in Figure 4.

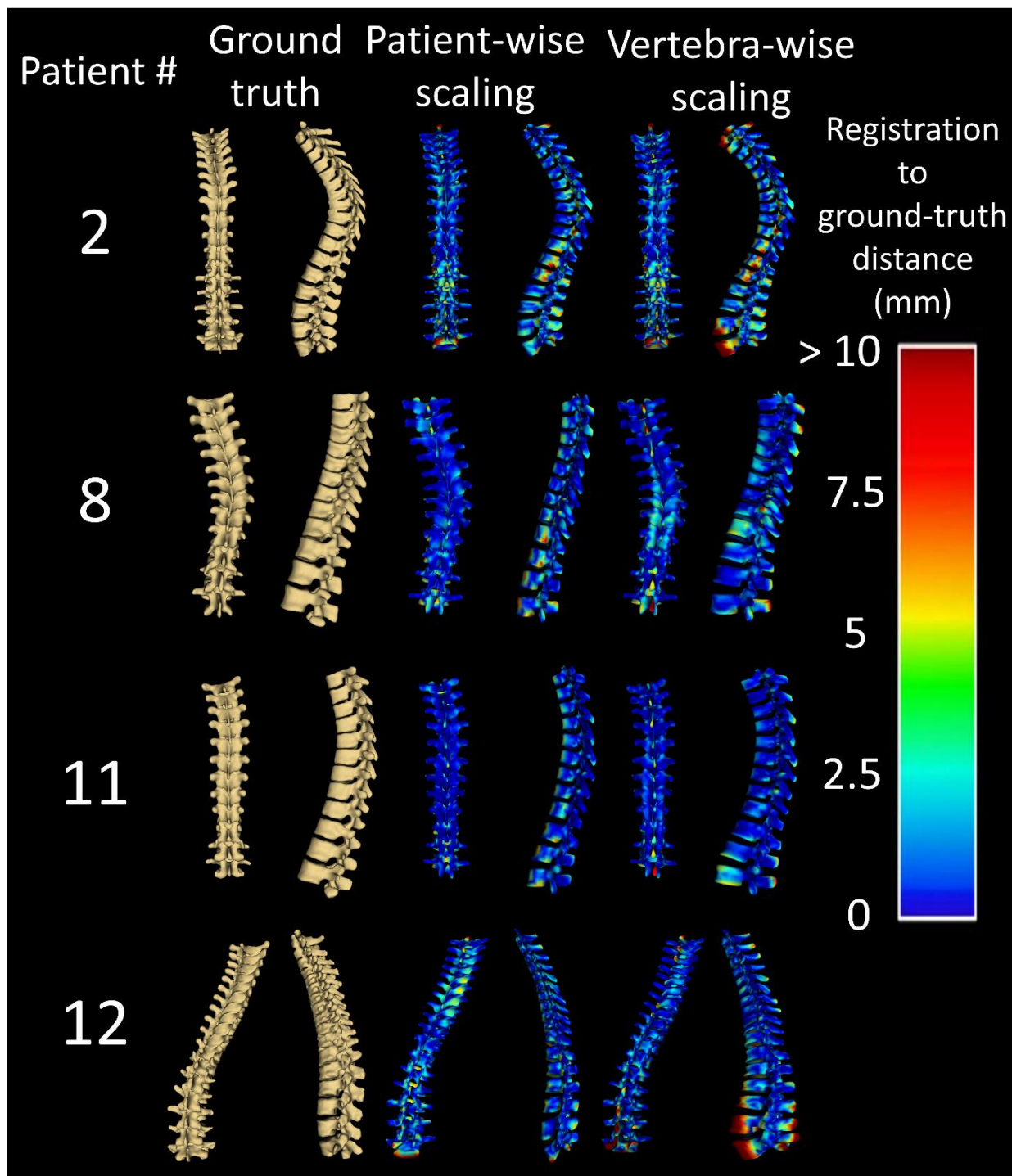


Figure 4: Error maps for four patients' registrations for the patient-wise scaling method from [Anon2017] and from the current vertebra-wise scaling method

4 Discussion

The registrations shown in Figure 4 provide some insight into the results in Table 1. The improvements seen in the average Hausdorff distances as a result of the proposed method appears to be the result of improved scaling of the vertebral bodies. The vertebral bodies of the registrations from our proposed method generally appear more realistic in scale than those resulting from patient-wise scaling. Since most of the volume of the spines are contained within the vertebral bodies, their improved scale decreased the mean average Hausdorff distance from 2.8mm to 2.3mm, or by about 18%.

Despite the modest decrease in the mean maximum Hausdorff distance from using vertebra-wise scaling, its standard deviation increased. This is likely due to two main factors: First, even if using patient-wise scaling produces less accurate registrations throughout its bulk, it scales the vertebrae consistently, whereas treating each vertebra individually allows for some vertebrae to deviate more in scale. These inaccurately scaled vertebrae, such as those at the ends of patients #2 and #12's spines result in large maximum Hausdorff distances without compromising the average Hausdorff distances, by virtue of the relatively small region affected. Secondly, the largest misalignments occur at the top and bottom boundaries of the spines where, despite the widening of the transverse processes, the vertebral bodies are not as large. Since for most vertebrae, wider transverse processes correspond to larger vertebrae, the deep learning models likely misinterpret the scales of these vertebrae at the ends of the patients' spines. Fortunately, misalignment in vertebral bodies does not compromise the utility of such registration for spinal injection navigation, as long as the posterior anatomy is accurately registered.

Further improvements in the vertebral scaling should be investigating, particularly for the lower lumbar and upper thoracic vertebrae, since these were the greatest source of error for the proposed method's registrations. These improvements might be achieved by using deep learning to predict the scales of patients' mid-thoracic to upper lumbar vertebrae, while using a composite method or imposing additional constraints for the problematic outer vertebrae. For instance, simply using the inter-landmarks distances to predict the scales of these vertebrae, similarly to [Anon2017] would reduce the error where it seems to under-predict their sizes. A natural idea is then to average the scale predicted by both methods for these vertebrae, expecting the over and under-prediction to cancel out.

More accurate registrations could also be achieved by improving the deep learning models' predictions. H2O offers a convenient hyper-parameter search framework in which a variety of model architectures can be generated systematically. The number of trials can be increased further by specifying multiple values for other network parameters, such as input dropout or regularization coefficients for example. Random geometric transforms can be probabilistically applied to the input vectors, before adding small amounts of noise to the landmark locations. Such data augmentation provides the models with more input samples, and improves generalization.

Before registrations produced using this method can be used for interventional navigation, their accuracy at the particular anatomic sites of interest must be validated. For facet joint injections, as an example, practitioners could locate these sites on both the registrations and their ground-truths. The distances between corresponding points identified on the ground-truths and registrations would serve to quantify the suitability of the registrations for navigation.

Furthermore, such registrations will need to be generated using landmarks collected from ultrasound scans. The transverse process locations used in this study were located from CT scan segmentations because of the large number available and their accuracy made them suitable for training the deep learning models, and provided ground-truths against which to compare the registrations. Until ultrasound data is used, the accuracy of intra-procedural registrations cannot be guaranteed to be sufficient for navigation.

5 Conclusions

The results presented in this work demonstrate the utility of the proposed method for producing registrations of abnormally shaped spines without the need for statistical shape atlases or ionizing radiation. The deep learning approach to vertebra-wise anatomic scale prediction proved to produce more accurate registrations than a patient-wise scaling approach. Nonetheless, practitioner-based validation of registrations produced from landmark locations collected from ultrasound is still required before this method can be implemented in practice.

References

- [Loizides2011] Loizides A, Peer S, Plaikner M, Spiss V, Galiano K, Obernauer J, Gruber H (2011) Ultrasound-guided injections in the lumbar spine. *Medical Ultrasonography* 13(1):54-8.
- [Ungi2012b] Ungi T, Abolmaesumi P, Jalal R, Welch M, Ayukawa I, Nagpal S, Lasso A, Jaeger M, Borshneck DP, Fichtinger G (2012) Spinal Needle Injection by Tracked Ultrasound Snapshots. *IEEE Transactions on Biomedical Engineering* 59(10):2766-72.
- [Nagpal2015] Nagpal S, Abolmaesumi P, Rasoulia A, Hacıhaliloğlu I, Ungi T, Osborn J, Lessoway VA, Rudan J, Jaeger M, Rohling RN, Borschneck DP, Mousavi P (2015) A multi-vertebrae CT to US registration of the lumbar spine in clinical data. *Int J CARS* 10:1371-81.
- [Zettinig2016] Zettinig O, Fuerst B, Kojcev R, Esposito M, Salehi M, Wein W, Rackerseder J, Sinibaldi E, Frisch B, Navab N (2016) Toward Real-time 3D Ultrasound Registration-based Visual Servoing for Interventional Navigation. *IEEE International Conference on Robotics and Automation*.
- [Behnami2016] Behnami D, Seitel A, Rasoulia A, Anas EMA, Lessoway V, Osborne J, Rohling R, Abolmaesumi P (2016) Joint registration of ultrasound, CT and a shape+pose statistical model of the lumbar spine for guiding anesthesia. *Int J CARS* 11:937-45.
- [Seitel2016] Seitel A, Sojoudi S, Osborne J, Rasoulia A, Nouranian S, Lessoway VA, Rohling RN, Abolmaesumi P (2016) Ultrasound-Guided Spine Anesthesia: Feasibility Study of a Guidance System. *Ultrasound in Med. & Biol.* 42(12): 3043-9.
- [Anon2017] Anonymous